Applied Catalysis B: Environmental 160–161 (2014) 445–455

Contents lists available at ScienceDirect

Applied Catalysis B: Environmental

journal homepage: www.elsevier.com/locate/apcatb

Phototransformation of model micropollutants in water samples by photocatalytic singlet oxygen production in heterogeneous medium

E. Díez-Mato[a], F.C. Cortezón-Tamarit[b], S. Bogialli[c], D. García-Fresnadillo[b,1], M.D. Marazuela[a,*,1]

[a] Dept. of Analytical Chemistry, Faculty of Chemistry, Universidad Complutense de Madrid, 28040 Madrid, Spain
[b] Dept. of Organic Chemistry, Faculty of Chemistry, Universidad Complutense de Madrid, 28040 Madrid, Spain
[c] Dept. of Chemistry, University of Padua, 35131 Padova, Italy

ARTICLE INFO

Article history:
Received 18 March 2014
Received in revised form 23 May 2014
Accepted 29 May 2014
Available online 6 June 2014

Keywords:
Micropollutants
Water treatment
Photocatalysis
Singlet oxygen
Ruthenium(II) Photosensitizers

ABSTRACT

The combination of photosensitized production of singlet oxygen ($^1O_2$) and solar energy is gaining increasing interest, as disinfection and water remediation technology. In this work, we have investigated the elimination of three common micropollutants such as, ibuprofen, paracetamol and bisphenol A using a photosensitizing material consisting of tris(4,7-diphenyl-1,10-phenanthroline)ruthenium(II) chloride, immobilized in a porous poly(dimethylsiloxane) inert support. The influence of variables such as, the radiation dose, hydrophobicity, ionization state of the micropollutant and water composition has been discussed.

The process has led to effective removal of ibuprofen and bisphenol A in ultra-pure water with conversion rates of 100% and 80%, respectively; whereas elimination of paracetamol was rather limited (35%). Experiments performed in natural water samples have evidenced reduced effectiveness of the $^1O_2$ photosensitized degradation process, due to water matrix composition. Thus, conversion rates of ibuprofen may decrease until 20% (depending on the water matrix) when other inorganic anions (e.g. bicarbonate, sulphate, etc.) are present in the water samples.

On the other hand, identification of the main transformation products of ibuprofen and bisphenol A has been achieved by the use of ultra-high-performance liquid chromatography-time-of-flight mass spectrometry (UHPLC/QTOF-MS). The phototransformation pathway of ibuprofen includes hydroxylation, decarboxylation and demethylation processes, while the degradation of bisphenol A mainly proceeded via fragmentation of the isopropylidene bridge between the two phenyl groups leading to different *para* substituted phenolic compounds.

© 2014 Elsevier B.V. All rights reserved.

1. Introduction

Currently unregulated chemicals, such as pharmaceutically active compounds (PhACs) and endocrine disrupting compounds (EDCs) have been found at low ng L^{-1} levels in environmental waters [1–4].

Among the most frequently occurred PhACs in surface waters are the anti-inflammatory (e.g. ibuprofen, IBP) and the analgesic drugs (e.g. paracetamol, PCT). Both groups of drugs are extensively used without prescription with an estimated annual consumption of several hundreds of tons in developed countries, and their presence in aquatic and surface water bodies has been detected at μg L^{-1} levels [5]. Although in the current European Water Framework Directive on Priority Substances [6] PhACs have not yet been regulated, a "first watch list" include diclofenac and future revisions of the EU Water Directive will include IBP and other drugs, among the list of substances with established drinking water limits.

On the other hand, the presence of EDCs in the aquatic environment has become an issue of considerable concern. EDCs comprise a large range of natural or synthetic substances that may interfere with the endocrine system -and in particular the sex hormones- of humans and animals. For instance, bisphenol A (BPA) is a molecule widely used in the industry for the synthesis of polycarbonate plastics and epoxy resins. Thus, BPA is widely found in effluents of wastewater treatment plants worldwide, as well as in groundwater and surface waters, so that it can be regarded as a good indicator of the industrial contribution of EDCs to wastewater [7,8].

The presence of organic pollutants in the aquatic environment, even at very low concentrations, suggests that existing

* Corresponding author. Tel.: +34 91 394 4217; fax: +34 91 394 4329.
E-mail address: marazuela@quim.ucm.es (M.D. Marazuela).
[1] Main author.

http://dx.doi.org/10.1016/j.apcatb.2014.05.050
0926-3373/© 2014 Elsevier B.V. All rights reserved.

Table 1
Chemical structure and physicochemical properties of the target pollutants.

Compound	Chemical structure	pK_a	log K_{ow}
Ibuprofen (IBP)	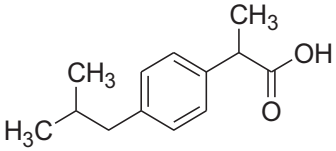	4.9	3.75/3.14[a]
Paracetamol (PCT)	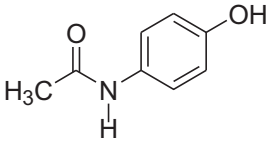	9.4	0.46
Bisphenol A (BPA)	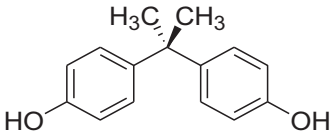	9.6–11.3	3.43

[a] Corresponding to the protonated and deprotonated IBP, respectively, and predicted by using the ACD/Labs Extension for CS ChemDraw (version 5.00) software.

wastewater treatment plants are not able to completely remove these substances. Therefore, efforts have to be directed towards the improvement and upgrade of conventional wastewater treatments for removal of micropollutants that cannot be readily eliminated at today's drinking water treatment facilities. One way of minimizing the input of micropollutants to surface waters is to integrate advanced treatment steps at wastewater treatment plants. The advanced treatment of effluents has been investigated using (photochemical) oxidation processes, membrane filtration or powdered activated carbon adsorption, among others [9,10].

Oxidation of micropollutants using photogenerated reactive oxygen species (ROS), such as singlet molecular oxygen ($^1O_2$) or superoxide radical anion ($O_2^{\bullet-}$) can proceed via the absorption of UV–vis radiation by a dye, the so called (photo)sensitizer, which photocatalyzes ROS production. After photoexcitation of the sensitizer to its excited triplet state, it can transfer its excitation energy to ubiquitous molecular oxygen leading to $^1O_2$ formation (a electrophilic chemical species), or it can transfer an electron to molecular oxygen producing $O_2^{\bullet-}$ which, in turn, can be involved in subsequent radical processes resulting in oxidation of organic substrates. Both photogenerated oxidizing species $^1O_2$ and $O_2^{\bullet-}$ are able to react with many of the organic pollutants commonly found in natural waters [11]. The application of photosensitized oxidation processes may be considered as one of the emerging green technologies for water treatment, due to the possibility of using two natural resources: dissolved oxygen and solar energy. However some disadvantages should be overcome, namely the low photostability of the sensitizers and the need to recover the dissolved sensitizer from the treated water. These drawbacks can be overcome by the use of stable photosensitizers [12] immobilized onto appropriate supports that will allow recycling the photosensitizer for further uses. Recent examples of the phototransformation of organic pollutants by supported photoactive $^1O_2$ generating agents, such as Rose Bengal, phthalocyanines, porphyrins and C_{60} aminofullerene derivatives have been described in the literature [13–17].

The aim of the present work was to study the transformation of model organic pollutants, namely IBP, PCT and BPA (Table 1) in aqueous solution, induced by oxidation with a $^1O_2$ photosensitizing material, which has been previously used in successful water disinfection treatments with compound parabolic collector (CPC) solar reactors [18,19]. Photosensitized oxidation experiments were performed in heterogeneous medium, using tris(4,7-diphenyl-1,10-phenanthroline)ruthenium(II) chloride (RDP^{2+}) as the singlet oxygen photosensitizer, immobilized in porous poly(dimethylsiloxane) membranes (pSil). Studies were performed, both in ultra-pure water and in different river water samples, in order to evaluate the influence of the matrix composition on pollutant's transformation efficiency.

Application of ultra-high-performance liquid chromatography-time-of-flight mass spectrometry (UHPLC/QTOF-MS) allowed us to identify the main transformation products (TPs) of IBP and BPA. Mono-hydroxylated IBP derivatives were detected among the first TPs, followed by a second step of demethylation and decarboxilation, leading to small molecular weight by-products. Break-up of the BPA molecule and further oxidation, results in different *para* substituted phenolic derivatives, such as 4-hydroxyacetophenone, 4-hydroxyphenyl-2-propanol and 4-hydroxybenzaldehyde as the main BPA phototransformation products.

2. Materials and methods

2.1. Reagents, solutions and photosensitizing material

The following analytical standards were used: ibuprofen monosodium salt (99.9%, Fluka, Buchs, Switzerland), paracetamol and bisphenol A (99.9%, Sigma–Aldrich, St. Louis, MO, USA), phosphoric acid (85%, Fluka, Buchs, Switzerland), sodium hydroxide (99%, Scharlau, Barcelona, Spain) and sodium azide (99.9%, Sigma–Aldrich, St. Louis, MO, USA). The singlet oxygen photosensitizer (RDP^{2+}) was synthesized according to the literature [21]. Deionized water used throughout all the experiments was obtained from Milli-Q water purification system (Millipore, Bedford, MA, USA). All solvents used for chromatographic analysis were provided by SDS (Peypin, France) and were HPLC grade.

Individual stock aqueous solutions of IBP, BPA and PCT were prepared at a concentration of 100 mg L^{-1} and stored at 4 °C. Working solutions of the target micropollutants with initial concentrations of 3 and 10 mg L^{-1} were prepared both, in ultra-pure water and in different river waters (Ebro, Segre and Valira rivers) collected at two different locations: the city of Logroño (153,137 inhabitants, 2012) and the village of Seo de Urgel (12,529 inhabitants, 2012), both in the region of the Ebro river basin (northeast of Spain) (Figure S1, Supplementary material). River water samples were collected in Pyrex borosilicate glass or PET containers. Once transported to the lab, samples were filtered through 0.22 μm nylon membranes (Scharlab, Barcelona, Spain) to remove suspended matter and stored in the dark at 4 °C until analysis. Finally, the river water

samples were spiked with the target compounds (at 3 mg L^{-1}) just before irradiation experiments in heterogeneous phase.

The photosensitizing material is composed of a singlet oxygen photosensitizer, tris(4,7-diphenyl-1,10-phenanthroline) ruthenium(II) dichloride ($^1O_2$ production quantum yield, Φ_Δ, 0.97 and 0.42 in deuterated methanol and water, respectively [20], immobilized in a poly(dimethylsiloxane) membrane (pSil) as the inert support (CulturSil, Cellon, Bereldange, Luxembourg) with two different sides: a porous one (0.5 mm thick porous silicone) and a smooth one (1.0 mm thick non-porous silicone). In order to increase the homogeneity of the photosensitizing material (reduction of dye precipitation on pSil surface) the RDP^{2+}/pSil membranes were prepared following a modified procedure compared to that previously described in the literature [18]. Briefly, 10 pSil membranes (3.5 × 150 cm) were boiled in deionized water for two hours. The hydrated membranes were refluxed overnight in the presence of a hydroalcoholic solution of RDP^{2+} (7.0×10^{-4} mol L^{-1}, in water/methanol, 8:2, v/v) and the dyed membranes were thoroughly washed with boiling water (3.4 L × 3 h × 6) in order to remove the weakly adsorbed photosensitizer. The dye concentration in the supernatant after the last washing under reflux was less than 10^{-9} mol L^{-1}, determined with a Varian Graphite Furnace GTA 110 atomic absorption spectrophotometer (Agilent Technologies, Madrid, Spain). Dye uptake by the pSil membranes was calculated from spectrophotometric measurements of the unbound sensitizer (ε_{461nm} = 32,400 L mol^{-1} cm^{-1} [20]) in the different washouts. This procedure gave a photosensitizer load of 0.97 ± 0.05 g m^{-2}. The resulting RDP^{2+}/pSil membranes were kept in zip-lock plastic bags until use.

2.2. Photosensitized oxidation experiments

Direct sunlight and $^1O_2$ mediated photosensitization experiments were performed at the rooftop of the Faculty of Chemistry in Madrid (latitude: 40° 24′N, longitude: 3°41′E), between 11:00 and 18:00 h during the months of May–July, 2012. The incident solar irradiation data all over this period were provided by the Spanish Agency for Meteorology (AEMET) at its UCM campus headquarters, (Figure S2, Supplementary material).

Direct photolysis experiments were carried out with individual aqueous solutions (10 mg L^{-1}, 3.5 mL) of IBP, PCT and BPA, contained in 1 × 1 cm polymethylmethacrylate cuvettes, useful in the wavelength range 280–800 nm (Scharlab, Barcelona, Spain) placed onto an orbital shaker and exposed to the sunlight radiation for several hours. Although typical environmental concentration of micropollutants are at ng L^{-1} level, we choose much higher initial concentrations for better evaluation of the $^1O_2$ photosensitized oxidation process and TPs identification. Singlet oxygen mediated phototransformation experiments were performed in a similar manner, but in the presence of small rectangular pieces (1.1 × 3.5 cm) of the photosensitizing material (RDP^{2+}/pSil) placed, with its porous side facing south, in the diagonal of the 1 × 1 cm polymethylmethacrylate cuvettes (Figure S3, Supplementary material). Dark control experiments for both direct and $^1O_2$ photosensitized oxidation studies were conducted in parallel. All experiments were performed by triplicate.

2.3. Photophysical characterization of the photosensitizing material

Steady-state and time-resolved luminescence measurements were performed with a SPT fluorometer (Horiba Fluoromax-4SPT, NJ, USA). Standard quartz cells (1 × 1 cm, Hellma 114-QS, Müllheim, Germany) equipped with a doubly-drilled septum cap were used. RDP^{2+}/pSil pieces (1.1 × 3.5 cm) were immersed in water, equilibrated with N_2 (C55, CarburosMetálicos, Madrid, Spain), O_2 (5.0, Praxair, Madrid, Spain) or air, respectively. The samples were placed in the diagonal of the cell, excited at 463 nm from the porous side and the emission from the same side was detected. The probability of excited-state quenching (Po_2^T) or fraction of triplet states of the sensitizer that are quenched by molecular oxygen in order to produce $^1O_2$ was calculated from steady-state emission measurements ($Po_2^T = 1 - (I/I_0)$), where I and I_0 are the luminescence intensities of the sensitizer in the presence and in the absence of oxygen, respectively). The emission lifetime of the photosensitizing material was measured with the Fluoromax-4SPT apparatus in its configuration for time-resolved emission measurements, with luminescence detection at 622 nm. The luminescence decay profiles were fitted to a 3-exponential function ($I_t = S + \Sigma B_i \exp(-t/\tau_i)$, i = 1, 2, 3; where I_t is the time dependent luminescence intensity, S the background signal, B_i the corresponding pre-exponential factors, and τ_i the individual lifetime components of the curve fit). The reduced weighted residuals (χ^2) and autocorrelation functions were employed to judge the goodness-of-the-fits. The pre-exponentially weighted mean lifetimes, τ_M ($\tau_M = \Sigma B_i \tau_i / \Sigma B_i$) were calculated from the experimental data. The $^1O_2$ lifetime was determined by detection of its characteristic phosphorescence at 1270 nm with an Edinburgh Instruments LP-900 laser flash photolysis system (Edinburgh, UK) equipped with a Nd-YAG laser (Minilite II, Continuum, CA, USA) for excitation at 532 nm (20 mJ per pulse), a film holder in a "magic angle" configuration for minimum light scattering detection, and a Hamamatsu H10330-45 NIR PMT (Iwata, Japan) for the time-resolved detection in the near-infrared. The emission spectrum of $^1O_2$ produced by the photosensitizing material was obtained by averaging 25 emission decays every 10 nm between 1200 and 1350 nm, using the time-resolved emission spectroscopy (TRES) acquisition mode included in the Edinburgh Instruments software package.

2.4. Analytical methodologies

Total organic carbon (TOC) and inorganic carbon (IC) content in the river water samples was measured by using a Shimadzu TOC-VCSH instrument (Tokyo, Japan). Conductivity and pH were measured with an Aqualytic conductimeter (Lódź, Poland) and a Crison GLP-22 pH meter (Barcelona, Spain), respectively.

After the scheduled irradiation time, the solutions of the target contaminants were analyzed by UV–vis spectroscopy, using a UV–vis Cary 1E spectrophotometer (Varian, Palo Alto, CA, USA). To monitor the evolution and concentration of the different analytes in each sample with respect to the irradiation time, a HP 1100 Series chromatographic system from Agilent Technologies (Palo Alto, CA, USA) was used. The instrument was equipped with a quaternary pump, on-line degasser, autosampler, automatic injector, a diode array detector (DAD) and a Kinetexpentafluorophenyl (PFP) "core-shell" column (100 × 4.6 mm, 2.6 μm) from Phenomenex (Torrance, CA, USA). The chromatographic analysis was performed in gradient mode with 10 mM phosphate buffer (pH 3.0) (solvent A) and acetonitrile (solvent B) at a flow rate of 1 mL min^{-1} and sample injection volume of 20 μL. Gradient conditions were as follows: 0–0.5 min, 45% B; 0.5–1.5 min, from 45 to 55% B; 1.5–5 min, 55% B, 5–6 min, from 55 to 45% B; 6–8 min, 45% B. The maximum absorption wavelengths used for quantification were: 220 nm (BPA and IBP) and 242 nm (PCT), respectively.

The TPs generated during the treatment process were monitored by a UHPLC/QTOF-MS system, equipped with a UHPLC apparatus (Agilent Series 1200; Agilent Technologies, Palo Alto, CA, USA), consisting of vacuum degasser, auto-sampler, a binary pump and a column oven coupled to both DAD and QTOF-MS mass analyzer (Agilent Series 6520; Agilent Technologies).

The chromatographic separation was performed on a Kinetex PFP column (100 × 2.1 mm, 2.6 μm, Phenomenex Torrance, CA, USA) thermostated at 25 °C, using water (solvent A) and acetonitrile (solvent B), at a flow rate of 0.2 mL min^{-1} and injecting 10 μL of sample. The elution gradient was linearly increased from 0 to 100% B in 10 min, and kept isocratic for 3 min, decreased back to 0% in 1 min and then finally kept isocratic for 6 min.

The QTOF system was equipped with an electrospray ionization interface (ESI), operating in dual ESI mode and negative ESI acquisition, with the following operation parameters: capillary voltage, 4000 V; nebulizer pressure, 35 psi; drying gas, 8 L min^{-1}; gas temperature, 350 °C; fragmentor voltage, 120 V; skimmer 65 V. Full scan mass spectra were recorded as centroid over the range 50–1000 *m*/*z* with a scan rate of 2 spectra/s. A QTOF calibration was daily performed with the manufacturer's solution. For all chromatographic runs the *m*/*z* 112.98558 corresponding to an adduct of formic acid, was set as reference mass for accurate mass analysis. The instrument provided a typical resolving power (FWHM) of about 18,000 at *m*/*z* 311.0805. Mass spectra acquisition and data analysis was processed with Masshunter Workstation B 04.00 software (Agilent Technologies, Palo Alto, CA, USA). A maximum deviation of ±5 ppm from a measured accurate mass with respect to the accurate mass possible elemental composition, calculated using the Elemental Composition Calculator embedded into the software was accepted.

3. Results and discussion

3.1. Ruthenium(II) complexes as $^1O_2$ photosensitizers

Ruthenium(II) complexes with polyazaheterocyclic chelating ligands of the 2,2′-bipyridine or 1,10-phenanthroline structural types have shown excellent properties to photosensitize the production of $^1O_2$ [20]. Some of the advantages displayed by this family of metal complexes are their higher photo- and thermal-stability compared to that of typical organic photosensitizers, such as Rose Bengal, methylene blue or phenalenone, and the feasibility of "fine tuning" their spectroscopic, photophysical and solubility properties by a judicious selection of the coordinating polyazaheterocyclic ligands. In addition, they can be easily immobilized on different types of polymer supports via covalent bonding, adsorption or electrostatic interactions [22]. In fact, these photosensitizers have been successfully applied to the development of photosensitizing materials for water disinfection with solar CPC reactors [18,19,21,23].

The $^1O_2$ photosensitizing material prepared in this work has a dye content of 0.97 ± 0.05 g m^{-2}. The excited state of the sensitizer in pSil membranes shows a luminescence band in the visible region (λ_{em}^{max} 622 nm). The probability of sensitizer excited-state quenching by oxygen (Po_2^T) under air-equilibrated conditions was calculated from steady-state emission measurements in the presence of Ar or air, respectively, and a probability of 0.76 ± 0.04 was determined; that means that 76% of the sensitizer triplet states are quenched by molecular oxygen (Figure S4, Supplementary material). Since the dye is immobilized in a microheterogeneous medium, time-resolved emission measurements allowed the calculation of the pre-exponentially weighted luminescence lifetime (τ_M) of the photosensitizing material in air-equilibrated water (Figure S5, Supplementary material). An averaged lifetime of 0.58 ± 0.06 μs was obtained. The Po_2^T and τ_M values for the photosensitizing material described in this work correlate well with those of similar photosensitizing materials described in previous literature works ($Po_2^T = 0.85$, $\tau_M = 0.48$ μs for a material loaded to saturation with a dye content of 2.0 g m^{-2} [21]; $Po_2^T = 0.75$, $\tau_M = 0.57$ μs for a recycled pSil membrane with a dye load of 0.30 g m^{-2} [19]. The $^1O_2$ emission lifetime measured in the photosensitizing material prepared in this work is 40 ± 4 μs (Figure S6, Supplementary material), in agreement with the $^1O_2$ lifetime values in the 30–40 μs range, previously determined for the RDP^{2+}sensitizer in pSil polymer [19,21].

One of the major problems associated with the use of any photosensitizing material in a solar reactor is its limited stability due to photobleaching, which reduces its efficiency and decreases its average span of life [24]. Immobilization of the photosensitizer on a solid support not necessarily guarantees enhanced stability. Thus, the effect of accumulated sunlight radiation on the RDP^{2+}/pSil membranes was firstly studied. Normalized emission intensity measurements of the immobilized photosensitizer show an 80% decrease after 15 hours of sunlight exposition, reaching a stable plateau at longer times which lasts for months after which the $^1O_2$ production by the photosensitizing material decreases to a level that excludes photodegradation of the water pollutants. This decrease in the efficiency of the photosensitizing material has been previously reported and can be attributed to sensitizer photobleaching due to dye oxidation, mainly at the ethylenic bridge sites of the 1,10-phenanthroline moieties, by the generated singlet oxygen [19,21]. Therefore, this type of photosensitizing material has a limited operational lifetime of ca. 6 months due to dye depletion [21]. However, the sunlight-exposed RDP^{2+}/pSil membranes can be reloaded with fresh RDP^{2+} sensitizer once it has been photobleached, as it has been demonstrated previously in disinfection studies [19]. The reloaded material has shown even better bactericidal efficiency than the original one, mainly attributed to photosensitizer aggregation on the surface of the porous silicone support. On the other hand, previous field tests have been performed with the same type of photosensitizing material, using solar reactors and natural water samples [25]. The efficiency of the photosensitizer strips was good during a testing period of three months. For longer times a partial loss of photosensitizer activity was observed, due to exhaustion of the photosensitizer and also to the water chemical composition. In fact, water samples with a rather large content of calcium and bicarbonate ions, as well as with relatively high pH would induce the formation of $CaCO_3$ deposits onto the surface of the membranes, which may limit the operational lifetime of the photosensitizing material.

3.2. Photosensitized experiments

It is worth mentioning that, in general, photooxidation of organic pollutants using $^1O_2$ rarely leads to complete mineralization of the organic compounds [24]. Instead, highly oxidized and/or degraded structures are commonly obtained, which may be less toxic and more suitable for subsequent biological treatment.

3.2.1. Experiments in ultra-pure water

Two types of experiments were carried out in ultra-pure water: (a) direct sunlight photodegradation and (b) photosensitized degradation via $^1O_2$ using RDP^{2+}/pSil membranes. Moreover, control runs with solutions of the micropollutants kept in the dark, in the absence and in the presence of the RDP^{2+}/pSil membranes, respectively, were performed to evaluate the stability of the solutions and/or the possible adsorption of the substrates to the polymer surface.

Pollutants are exposed to natural sunlight in surface waters; therefore direct photolysis might be a significant pathway for pollutants transformation. However, the results depicted in Fig. 1 demonstrate that none of the target pollutants are photodegraded by sunlight. This can be explained by the fact that IBP, PCT and BPA show poor absorption in the wavelength region of the solar spectrum (λ > 280 nm, Figure S7 Supplementary material) and, in consequence, they do not suffer transformation by direct photolysis. Furthermore, dark control experiments performed to rule out

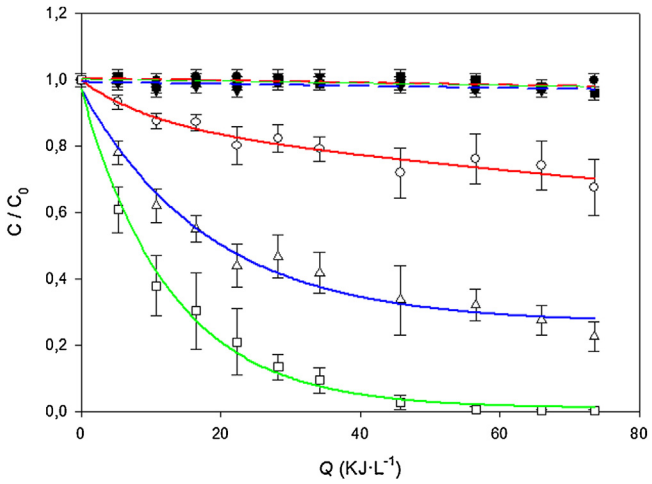

Fig. 1. Results of the single-compound photodegradation experiments. Direct photolysis of PCT (●), BPA (▼) and IBP (■) and photosensitized degradation via $^1O_2$ of PCT (○), BPA (△) and IBP (□). C_0 = 10 mg L^{-1}. Each point corresponds to the mean of three replicates.

the possible hydrolysis of the pollutants showed that their concentrations did not significantly change after seven hours.

Hence, the selected compounds were subjected to photosensitized degradation with $^1O_2$ which, due to its electrophilic character, reacts readily with electron-rich organic substrates bearing functional groups such as activated double bonds, phenols or sulfides.

The experiments were performed by irradiating ultra-pure water solutions of each contaminant separately (single-compound experiments) or all three in the same solution (mixture experiments), in the presence of the RDP^{2+}/pSil membranes. In single-compound experiments, the UV spectra of the solutions irradiated at different times were registered. The results shown in Fig. 2 display that the UV spectra of IBP and BPA aqueous solutions changed significantly after photosensitized sunlight exposition for seven hours, suggesting their transformation in other chemical species; whereas the observed changes in the irradiated PCT solutions were not so dramatic. Moreover, the chromatographic analysis of the irradiated solutions revealed the progressive disappearance of the target contaminants and the appearance of unknown transformation products at low retention times (Figure S8, Supplementary material).

On the other hand, Fig. 1 shows the degradation curves obtained for each compound in ultra-pure water, as a function of the accumulated solar energy (Q) per volume unit along the experiment. Q is used instead of the experimental time; because this is a convenient way to normalize the intrinsically variable conditions of sunlight irradiance during one-day experimental periods (see Figure S2, Supplementary material). The parameter Q (kJ L^{-1}) was calculated according to the following equation:

$$Q = \sum_{i=0}^{n} \left(\frac{A \times \Delta t \times E_0}{V_T} \right)_{t_i} \quad (1)$$

where A (m^2) is the area of photosensitizing material under solar irradiation; V_T (L) is the volume of the treated solution; E_0 is the averaged fluence rate of the incident solar radiation (kJ s^{-1} m^{-2}) for a time interval Δt (s) between two sampling times (i).

Although some authors have claimed that ibuprofen does not contain functional groups susceptible to singlet oxygen reactivity [26], the degradation curves in Fig. 1 show that accumulated sunlight radiation (Q) doses between 50 and 60 kJ L^{-1} (corresponding to 4–5 h of solar exposition in a typical sunny day) led to total disappearance of IBP; whereas conversion rates for BPA and PCT were

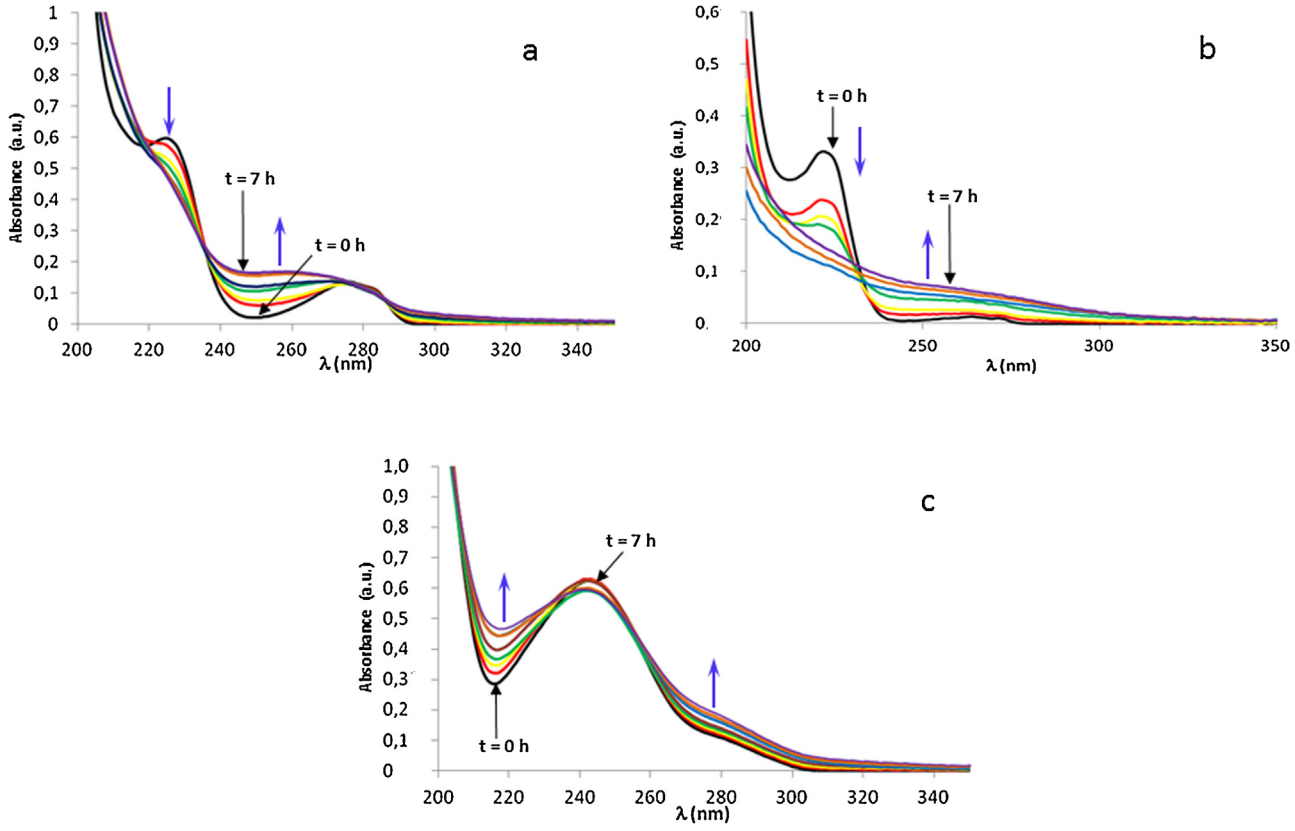

Fig. 2. Absorption spectra changes observed during $^1O_2$ photosensitized degradation of aqueous solutions of: (a) BPA, (b) IBP and (c) PCT.

80% and 35%, respectively. An explanation for these results may be the different hydrophobicity ($\log K_{ow}$) and acidity constants (pK_a) of the different compounds, summarized in Table 1.

Singlet molecular oxygen is short-lived chemical species in water, with a lifetime in the 3–5 μs range, so that $^1O_2$ diffusion is restricted to approximately 0.1 μm away from the polymer surface, once the oxygen molecule in its excited state escapes the photosensitizing material and reaches the aqueous phase [18,21]. Therefore, in heterogeneous media, those species in close proximity to the photosensitizing material will be subjected to the oxidizing effect of $^1O_2$. In other words, depending on the hydrophobicity and the ionization state of the different pollutants, each compound will interact to a different extent with the photosensitizing material where the $^1O_2$ is photogenerated, and those organic substrates better adsorbed on the RDP^{2+}/pSil membranes will suffer enhanced photodegradation.

As far as IBP concerns, under most conditions that are relevant to surface waters, IBP exists predominantly in its deprotonated form, because of its low pK_a value (4.9). IBP anion is also slightly more hydrophilic than its protonated form (Table 1). However, the attractive electrostatic interactions between the deprotonated IBP and the RDP^{2+} cationic photosensitizer, together with the hydrophobic interactions with pSil, can favor its adsorption on the membrane and, consequently, its photodegradation process by $^1O_2$. On the other hand, phenolic compounds such as, BPA and PCT have shown lower reactivity toward $^1O_2$ in their protonated form (which is the predominant one at neutral pH) compared to the phenolate form [15].

Thus, in ultra-pure water only the hydrophobic interactions will favor adsorption of BPA ($\log K_{ow} = 3.43$; $pK_a = 9.4$) onto the RDP^{2+}/pSil membranes. This fact facilitates its photodegradation by $^1O_2$, although to a minor extent than that of IBP which is compatible with the lower reactivity of protonated phenols toward $^1O_2$. Finally, PCT ($\log K_{ow} = 0.46$; $pK_a = 9.6–11.3$) which is quantitatively protonated at neutral pH and is the most hydrophilic compound of the series, will be less adsorbed on the membrane surface and, therefore, poorly photodegraded. A similar enhanced local concentration effect has been described for other supported photosensitizers and substrates [13,27,28].

These hypotheses were confirmed with "blank" experiments carried out with individual aqueous solutions of the target compounds, kept in the dark for several hours in the presence of the porous RDP^{2+}/pSil membranes. No significant changes in PCT concentration were found, whereas the IBP and BPA levels decreased to approximately 85% of the initial values (Figure S9, Supplementary material). These results can be attributed to a more efficient adsorption of IBP and BPA onto the photosensitizing material and they evidence that proximity between the photosensitizer and the target compound is essential to achieve photodegradation.

Furthermore, $^1O_2$ quenching experiments were carried out in order to confirm that reaction with $^1O_2$ is the dominating pathway of degradation. Thus, photosensitized degradation of IBP solutions was performed, both in the absence and in the presence of sodium azide (NaN_3), a well-known $^1O_2$ quencher [29]. The results depicted in Fig. 3 indicate that in the presence of NaN_3, photosensitized degradation of IBP is significantly inhibited and the observed concentration decay is equivalent to the adsorption of the analyte onto the photosensitizing material, as observed in blank experiments (Figure S9, Supplementary material). Therefore, it can be assumed that the reaction with $^1O_2$ is the only photochemical pathway that causes IBP degradation.

On the other hand, synergistic or antagonistic effects can be observed in complex mixtures of pollutants and their photoproducts [30]. Therefore, $^1O_2$ mediated phototransformation experiments with all three compounds in the same solution ($C_0 = 3\ mg\ L^{-1}$ each) were also performed, as it occurs in nature or during wastewater and surface water treatment. In this case, no significant differences in terms of conversion rates of the different compounds have been observed with respect to the individual experiments (data not shown). An explanation for this fact can be found taking into account that: (i) $^1O_2$ production by the photosensitizing material is not a limiting factor [19]; (ii) the total concentration of the pollutants is not significantly higher than that used in individual experiments and, (iii) the reactivity of PCT towards $^1O_2$ is low, so that it does not affect the observed conversion rates of IBP and BPA substrates, which are more reactive towards singlet oxygen.

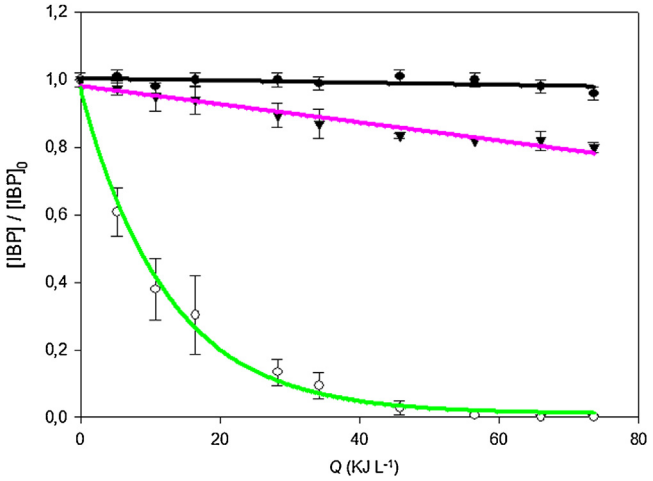

Fig. 3. Comparison of the degradation curves of solutions of IBP ($C_0 = 10\ mg\ L^{-1}$ in Milli-Q water) caused by direct photolysis (●), photosensitized oxidation via $^1O_2$ (○) and photosensitized oxidation via $^1O_2$ in the presence of NaN_3 (50 mM) (▼). Each point corresponds to the mean of three replicates.

3.2.2. Experiments in river water samples

The effectiveness of the phototransformation process might be affected by the composition of the raw water [15], in particular due to the presence of particulate or dissolved organic matter and dissolved inorganic ions, so the influence of water matrix composition on the degradation efficiency was evaluated using different river water samples (Table 2). The samples were collected in two locations along the Ebro river basin. Both sampling locations represent two different domains within the Ebro river basin, in terms of geological and geographic environments, population, and presence of industrial or agricultural activities which influence the chemical composition of freshwaters collected in those places. As shown in Table 2, the main difference is found in the inorganic carbon content and the conductivity values, which give an idea of the total ion content. Thus, typical composition of Segre and Valira water sources is dominated by the presence of calcium and bicarbonate ions (around 70% each), whereas natural composition of river waters collected in the northwest part of the Ebro river basin include other majority ions like sulphate and chloride, besides calcium and bicarbonate [31].

Fig. 4 shows the phototransformation curves of the different substrates obtained in river waters, compared to those obtained in ultra-pure water. Moreover, Table 3 collects a summary of the results obtained for the selected compounds, in terms of both, degradation rates and pseudo-first-order apparent rate constants (k_{app}) which were calculated according to Equation (2):

$$\ln \frac{C_t}{C_0} = -k_{app} \times t \quad (2)$$

where t is the irradiation time, and C_0 and C_t are the concentration of the substrates at irradiation time zero and t, respectively.

Table 2
Physicochemical quality parameters measured in target waters.

	pH	TOC[a] (mg L^{-1})	IC[b] (mg L^{-1})	Conductivity (25 °C) (μS cm^{-1})
Milli-Q water	5.60 ± 0.01	0.00	0.00	1.1 ± 0.1
Ebro river (Logroño)	8.13 ± 0.01	1.6 ± 0.3	38.4 ± 3.4	478 ± 4
Segre river (Seo de Urgel)	7.45 ± 0.01	1.8 ± 0.1	8.8 ± 0.1	134 ± 1
Valira river (Seo de Urgel)	7.70 ± 0.01	1.0 ± 0.2	14.0 ± 0.1	196 ± 2

[a] Total organic carbon.
[b] Inorganic carbon.

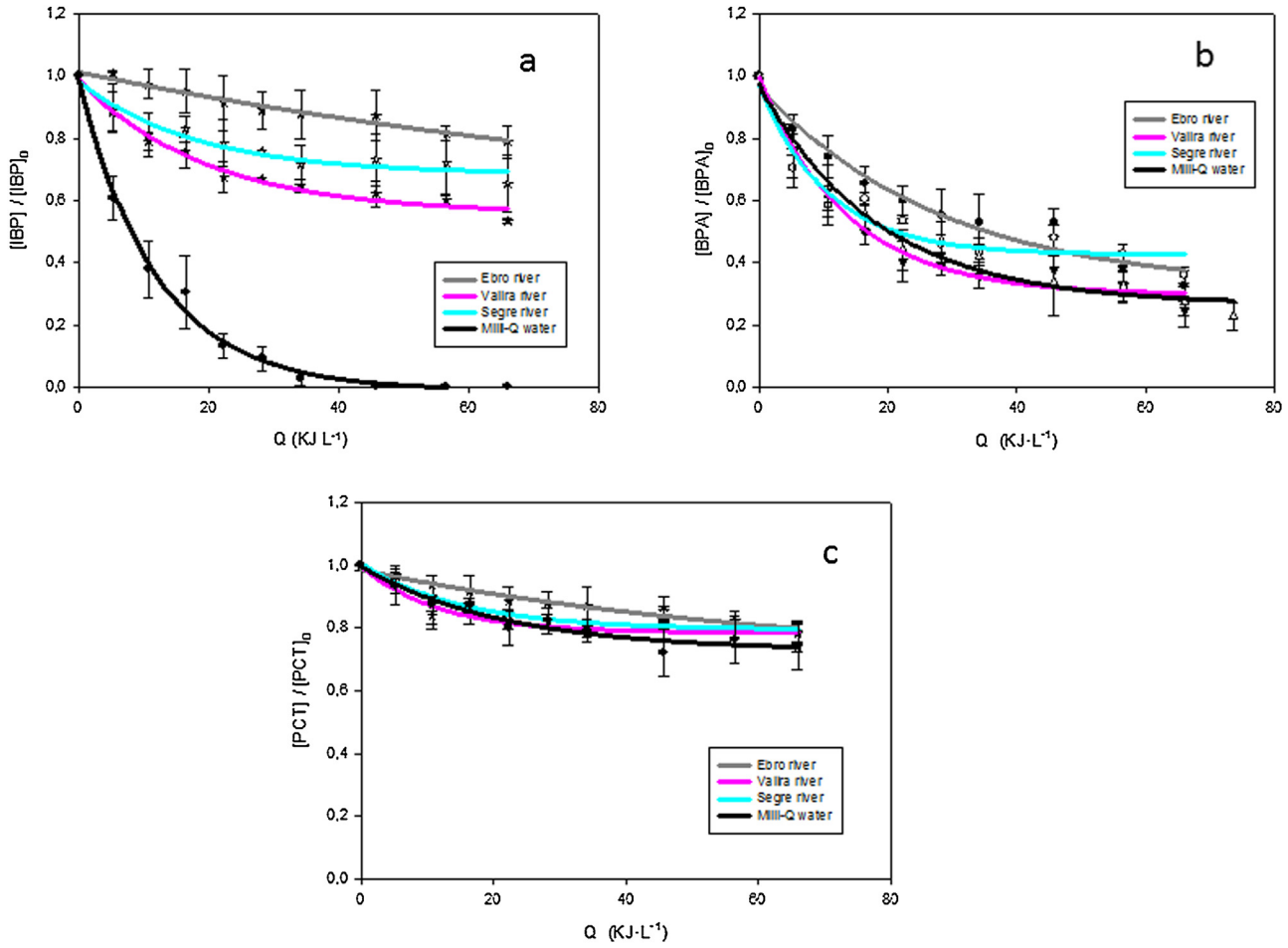

Fig. 4. Comparison of $^1O_2$ photosensitized degradation curves of: (a) IBP, (b) BPA and (c) PCT in Milli-Q and river waters (C_0 = 3 mg L^{-1}). Each point corresponds to the mean of three replicates.

The comparison of pseudo-fist-order rate constants for photosensitized degradation in ultra-pure water and river water samples (Table 3) shows moderate loss of photosensitizing activity under real samples condition. For instance, the degradation rates and k_{app} of IBP in all river waters tested, are appreciably lower than in ultra-pure water. The explanation for these results might be a combination of two factors: firstly, the presence of dissolved organic matter that scavenge photochemically generated $^1O_2$ to a certain degree and secondly, the competition between the anionic IBP (which prevails at the pH values of surface waters) and other inorganic species (e.g. bicarbonate, sulphate and chloride present in the natural waters) for the cationic sites on the surface of the

Table 3
Comparative study of photosensitized $^1O_2$ degradation experiments in different aqueous matrices.[a]

Sample	IBP		BPA		PCT	
	Conversion rate (%)	k_{app} (h^{-1})	Conversion rate (%)	k_{app} (h^{-1})	Conversion rate (%)	k_{app} (h^{-1})
Milli-Q water	100	0.920 ± 0.044	80	0.174 ± 0.011	35	0.042 ± 0.004
Ebro river	20	0.041 ± 0.002	60	0.173 ± 0.010	20	0.037 ± 0.002
Segre river	30	0.056 ± 0.009	55	0.103 ± 0.011	20	0.030 ± 0.006
Valira river	40	0.090 ± 0.011	70	0.178 ± 0.024	20	0.032 ± 0.007

[a] The reported errors in k_{app} were estimated by curve fitting to first order kinetics.

Table 4
Accurate mass measurements of the TPs of IBP and BPA as determined by UHPLC/QTOF-MS.

Compound	t_R (min)	Molecular formula	Theoretical $[M-H]^-$, (m/z)	Experimental $[M-H]^-$, (m/z)	Error (mDa)
IBP	11.05	$C_{13}H_{18}O_2$	205.1234	205.1222	−1.2
IBP-TP1	9.15	$C_{13}H_{16}O_4$	235.0976	235.0968	−0.8
IBP-TP2	8.94	$C_{13}H_{18}O_3$	221.1183	221.1176	−0.8
IBP-TP3	8.65	$C_7H_6O_2$	121.0295	121.0294	−0.1
IBP-TP4	4.47	$C_6H_{10}O_4$	145.0506	145.0501	−0.5
BPA	10.33	$C_{15}H_{16}O_2$	227.1078	227.1064	−1.4
BPA-TP1	7.41	$C_9H_{12}O_2$	151.0765	151.0757	−0.8
BPA-TP2	8.28	$C_8H_8O_2$	135.0452	135.0446	−1.5
BPA-TP3	8.57	$C_7H_6O_2$	121.0295	121.0292	−0.3

photosensitizing material. This process can limit effective adsorption of IBP on the membrane surface, where $^1O_2$ is produced, causing a decrease of the degradation rate. In fact, the results obtained correlate well with this hypothesis, since conversion rates for IBP dropped to 20% in the Ebro river sample, which has the highest conductivity and inorganic carbon content (Table 2).

On the other hand, it has been reported that oxidation of BPA by OH• radical-based processes (e.g. Fenton) is completely inhibited by the presence of certain inorganic ions (e.g. bicarbonate) that act as scavengers towards OH• [32]. By contrast, photosensitized degradation of BPA is slightly reduced but not inhibited in natural waters, as it can be observed in the data summarized in Table 3. Phenols like BPA are highly reactive with $^1O_2$ [33] because the hydroxyl substituents increase the electron donor ability of the aromatic compound towards the electrophilic $^1O_2$ and, conversely to IBP, do not show any ionization at the normal pH values of natural waters, so that differences between ultra-pure and river water matrices are not so dramatic.

Finally, PCT is the substrate with the lowest conversion rates of all three (between 20 and 35%) and the water matrix composition seems to have negligible effects on its photodegradation efficiency. Being PCT the most hydrophilic species and having a pK_a of 9.6–11.3, it will be little adsorbed on the surface of the photosensitizing material and therefore, poorly degraded by the $^1O_2$ within its lifetime.

3.2.3. *Identification of the TPs of IBP and BPA by UHPLC/QTOF-MS*

It has to be taken into account that the chromatograms obtained from $^1O_2$ degradation experiments of IBP and BPA aqueous solutions are rather complex, showing several small peaks at shorter retention times than the parent compound, suggesting the formation of smaller and more polar TPs. In this study we focused mostly on the identification of the main transformation products. The high resolution and mass accuracy measurements provided by the QTOF analyzer allowed the assignment of highly probable molecular formulae with a mass error ≤1.5 mDa (Table 4).

Fig. 5 shows the TPs of IBP and BPA, hypothesized on the basis of UHPLC/QTOF-MS results. Concerning IBP, hydroxylation seems to be the first step of $^1O_2$ induced phototransformation. This hypothesis is supported by two characteristic anions, namely m/z of 235.0968 (**IBP-TP1**) and 221.1191 (**IBP-TP2**), respectively (Fig. 6a) that correspond to keto-mono-hydroxylated and

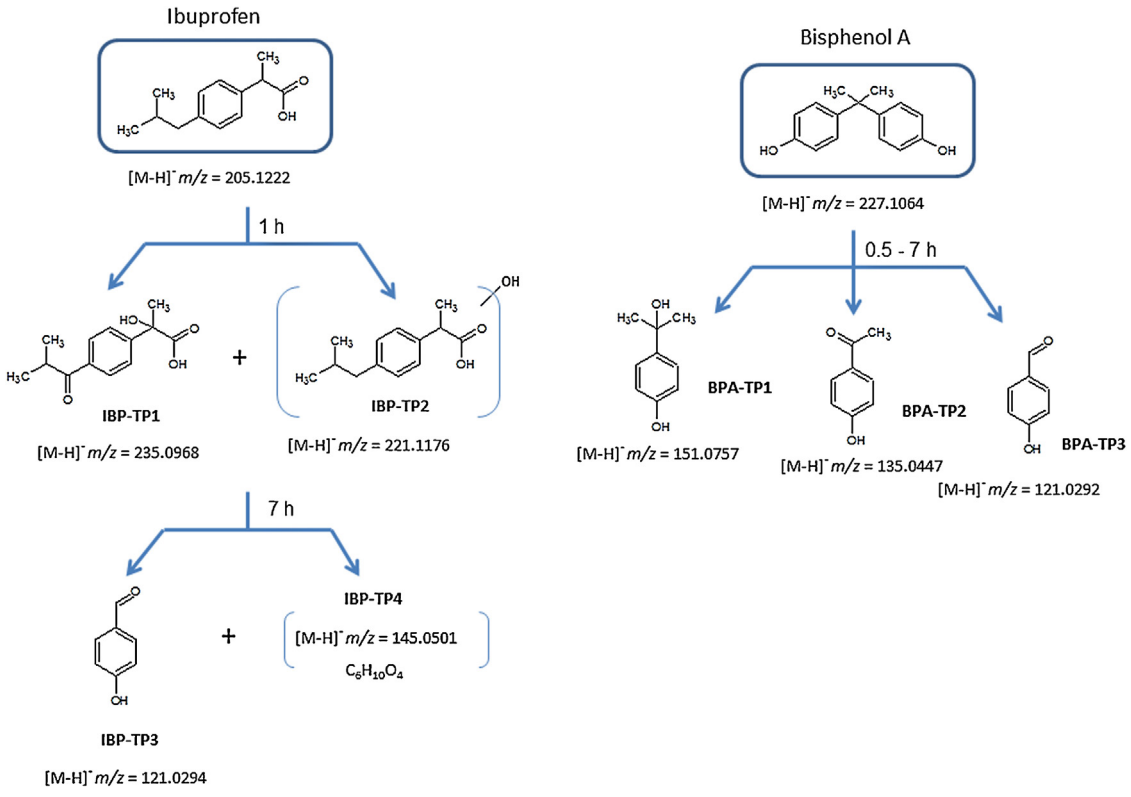

Fig. 5. Identified transformation products of IBP and BPA as determined by UHPLC/QTOF-MS.

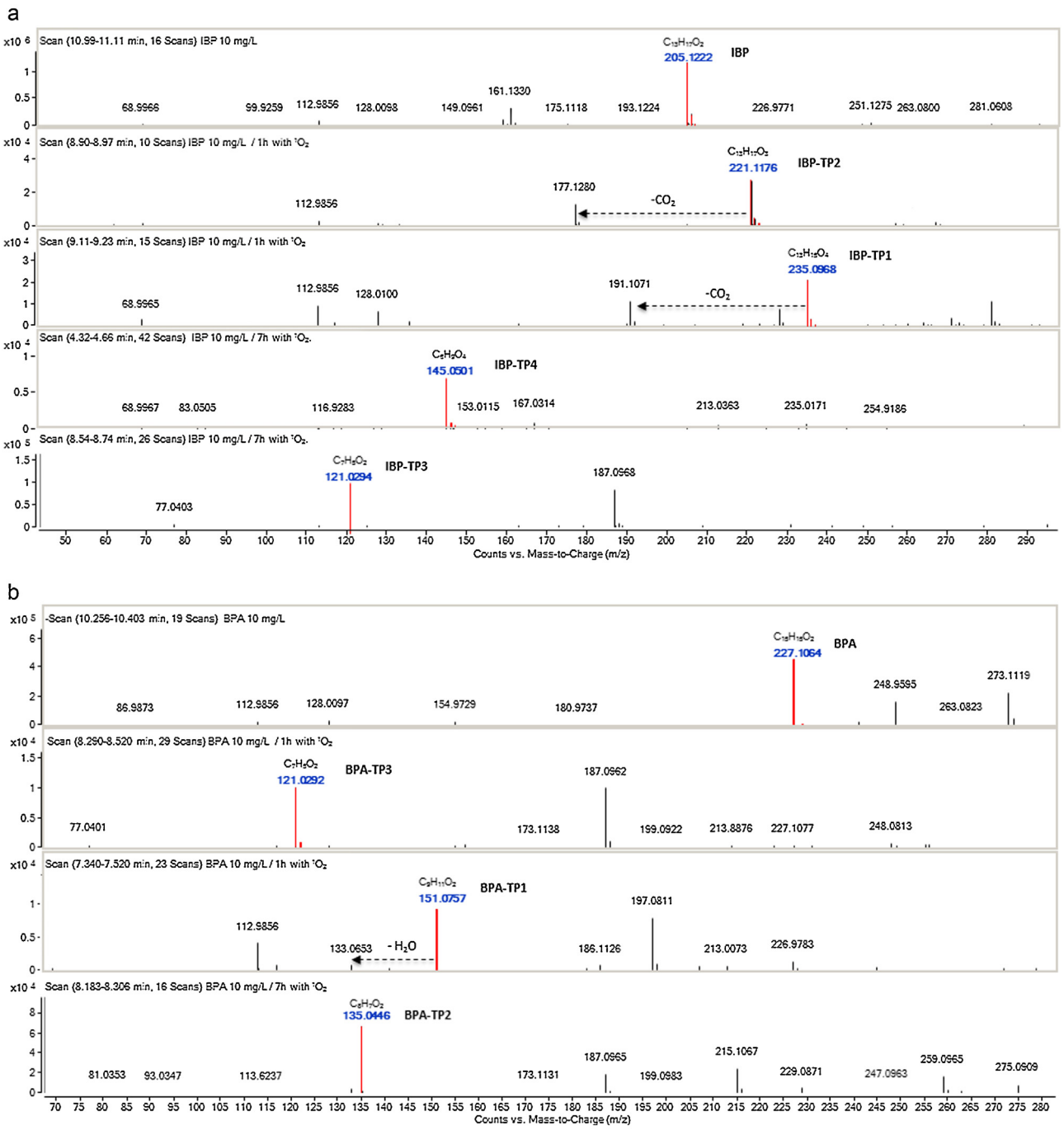

Fig. 6. Accurate ESI(−)/QTOF-MS mass spectra of: (a) IBP and its TPs and (b) BPA and its TPs.

mono-hydroxylated derivatives. These are the main IBP-TPs at the lowest *Q* doses (corresponding to 1–2 h of solar exposition in a typical sunny day). In addition, IBP-TP1 and IBP-TP2 show in-source fragmentation producing $[M\text{-}H\text{-}CO_2]^-$ ions with *m*/*z* of 191.1071 and 177.1280, respectively (Fig. 6a), evidencing the presence of the carboxylic acid group.

Actually, the structure of IBP-TP2 can be attributed to different hydroxy-IBP positional isomers, corresponding to either, hydroxylation on the side chains of the molecule or on the aromatic ring. The first option can lead to 1-hydroxy-IBP or 2-hydroxy-IBP, among others, which are also reported as products of human metabolite and biotransformation of the parent compound [34,35]; although some authors have recently concluded that hydroxylation of the aromatic ring is of high importance [36,37].

The formation of mono-hydroxylated derivatives has also been reported in the degradation of IBP by (photoelectro)-Fenton [38,39], heterogenous Fenton-like reactions [40], (sono)-photocatalysis [37,41–43] and γ-irradiation [36,44] treatments.

Following hydroxylation, $^1O_2$ mediated-phototransformation of IBP at higher *Q* doses (typically 7 h of solar irradiation) continues with demethylation or decarboxylation processes. Thus, two different TPs, namely **IBP-TP3** and **IBP-TP4** (Fig. 5) with experimental *m*/*z* values of 121.0294 and 145.0499, respectively (Fig. 6a) have been detected.

The ion [M-H]$^-$ m/z 121 has also been observed in IBP degradation studies, using (sono)-photocatalysis [43] and γ-irradiation [44] and in both cases, it was attributed to 4-ethylphenol ($C_8H_{10}O$). However, the accurate mass measurements provided by the QTOF analyzer has allowed to assign the measured [M-H]$^-$ m/z 121.0294 to the best-fit formula of $C_7H_6O_2$ (theoretical [M-H]$^-$ m/z 121.0295, error −0.1 mDa), that may correspond to both, 4-hydroxybenzaldehyde or benzoic acid. Nevertheless, a standard of benzoic acid injected under the assayed chromatographic conditions elutes at 2.81 min, very different of IBP-TP3 retention time (8.65 min), so it can be finally assigned to 4-hydroxybenzaldehyde.

The presumable structure of IBP-TP4 (best-fit formula of $C_6H_{10}O_4$) could not be determined, based on the available information.

To the best of our knowledge, IBP-TP1 and IBP-TP3 have not been previously found in other advanced oxidation or biotransformation studies of IBP. Experiments aimed to evaluate the potential toxicity of the TPs have not been performed so far in this work; however, reported data about lethal dosage values (LD50 oral-rat) for IBP and its TPs, IBP-TP2 and IBP-TP3, correspond to 636 mg kg^{-1}, 980 mg kg^{-1} and 2.25 g kg^{-1}, respectively [45]. Therefore, the IBP-TP2 and IBP-TP3 photoproducts are less toxic than their parent compound.

In the case of BPA, fragmentation and oxidation leads to different *para* substituted phenols. The product (**BPA-TP1**) with an accurate mass of [M-H]$^-$ m/z of 151.0757 (Table 4) is identified as 4-hydroxyphenyl-2-propanol ($C_9H_{12}O_2$), generated by cleavage of the single bond between the isopropylidene carbon and the phenyl group of BPA, confirming previous observations [46,47].

Previously reported studies involving Fenton, (sono)-photocatalytic or photosensitized degradation of BPA [32,33,46,48,49] have equally assigned the ion [M-H]$^-$$m/z$ 135 to 4-hydroxyacetophenone ($C_8H_8O_2$), or to an isobaric compound 4-isopropylphenol ($C_9H_{12}O$); however none of these works use high-resolution accurate mass spectrometry.

The accurate mass measurements provided by the QTOF analyzer has allowed us to unequivocally assign the measured [M-H]$^-$ m/z 135.0446 to the best-fit formula of $C_8H_8O_2$ (theoretical [M-H]$^-$, m/z 135.0452, error −1.5 mDa), that corresponds to 4-hydroxyacetophenone (**BPA-TP2**).

Another TP was identified as 4-hydroxybenzaldehyde (**BPA-TP3**) at experimental m/z 121.0292 that is probably formed in a secondary step from either or both intermediates (**BPA-TP1**, **BPA-TP2**).

The LD50 values for BPA and some of its TPs (BPA-TP2 and BPA-TP3) correspond to 5 g kg^{-1}, 1.5 g kg^{-1} and 2.25 g kg^{-1}, respectively [45]. According to these values, BPA-TP2 and BPA-TP3 are more toxic compared to the parent BPA substrate; however, both BPA-TPs exhibit slight estrogenic activity compared to that of BPA itself [50].

4. Conclusions

The presence of micropollutants in surface waters has become a problem of environmental and health concern. This work reports a phototransformation study of three water micropollutants, namely IBP, BPA and PCT, using a $^1O_2$ photosensitizing material and solar energy. The $^1O_2$ photosensitizing material, which can be used in compound parabolic collector solar reactors, has been photophysically characterized.

From the results shown herein, it can be concluded that all target analytes are not amenable to phototransformation, under usual environmental conditions (direct photolysis).

Concerning $^1O_2$ photosensitized degradation experiments performed in ultra-pure water; the three analytes show different behavior. IBP is eliminated more efficiently, followed by BPA; whereas PCT shows reluctance to react with $^1O_2$. PCT is the most hydrophilic compound of the series and it is quantitatively protonated at neutral pH. Therefore, it is less adsorbed on the membrane surface where $^1O_2$ is produced and consequently, poorly photodegraded.

This hypothesis was confirmed with "blank" experiments carried out with individual solutions of the target compounds, kept in the dark for several hours in the presence of the porous RDP^{2+}/pSil membranes.

On the other hand, the matrix effect observed in experiments performed in river water samples can be attributed to the presence of dissolved organic matter and other inorganic ions (e.g. bicarbonate, sulphate, etc.), that compete with the organic substrates for the $^1O_2$ and for the cationic sites on the surface of the photosensitizing material, respectively.

The main TPs resulting from photosensitized degradation of IBP and BPA, have been structurally elucidated by UHPLC/QTOF-MS. Hence, photosensitized degradation of IBP generates firstly, hydroxylated-IBP derivatives followed by successive demethylation/decarboxylation steps, leading to smaller fragments. Degradation of BPA occurs via break-up of the molecule through the isopropylidene group and further oxidation, yielding to different *para* substituted phenolic intermediates.

Acknowledgements

M.D.M. gratefully acknowledges the financial support of the University of Padua for a short-term stage as Visiting Scientist in the Department of Chemistry.

Appendix A. Supplementary data

Supplementary data associated with this article can be found, in the online version, at http://dx.doi.org/10.1016/j.apcatb.2014.05.050.

References

[1] K.E. Murray, S.M. Thomas, A.A. Bodour, Environ. Pollut. 158 (2010) 3462–3471.
[2] S.D. Richardson, Anal. Chem. 81 (2009) 4645–4677.
[3] C.G. Daughton, Contaminants of Emerging Concern in the Environment: Ecological and Human Health Considerations, in: R. Halden (Ed.), ACS Symposium Series, American Chemical Society, Washington DC, 2010, pp. 9–68.
[4] M.D. Celiz, J. Tso, D.S. Aga, Environ. Toxicol. Chem. 28 (2009) 2473–2484.
[5] A. Ziylan, N.H. Ince, J. Hazard. Mater. 187 (2011) 24–36.
[6] Directive 2013/39/EU of the European Parliament and of the Council of 12th August 2013, amending Directives 2000/60/EC and 2008/105/EC as regards priority substances in the field of water policy Text with EEA relevance, OJ L 226, 24.8 (2013), pp. 1–17.
[7] M. Stuart, D. Lapworth, E. Crane, A. Hart, Sci. Total Environ. 416 (2012) 1–21.
[8] D.W. Hawker, J.L. Cumming, P.A. Neale, M.E. Bartkow, B.I. Escher, Water Res. 45 (2011) 768–780.
[9] M. Klavaroti, D. Mantzavinos, D. Kassinos, Environ. Int. 35 (2009) 402–417.
[10] I. Oller, S. Malato, J.A. Sánchez-Pérez, Sci. Total Environ. 409 (2011) 4141–4166.
[11] D. Gryglik, J.S. Miller, S. Ledakowicz, J. Hazard. Mater. 146 (2007) 502–507.
[12] M.C. DeRosa, R.J. Crutchley, Coord. Chem. Rev. 233–234 (2002) 351–371.
[13] V. Fabregat, M.I. Burguete, F. Galindo, S.V. Luis, Environ. Sci. Pollut. Res. (2014), http://dx.doi.org/10.1007/s11356-013-2311-8.
[14] M. Silva, M.J.F. Calvete, N.P.F. Goncalves, H.D. Burrows, M. Sarakha, A. Fernandes, M.F. Ribeiro, M.E. Azenha, M.M. Pereira, J. Hazard. Mater. 233–234 (2012) 79–88.
[15] H. Kim, W. Kim, Y. Mackeyev, G.S. Lee, H.J. Kim, T. Tachikawa, S. Hong, S. Lee, J. Kim, L.J. Wilson, T. Majima, P.J.J. Alvarez, W. Choi, J. Lee, Environ. Sci. Technol. 46 (2012) 9606–9613.
[16] J. Kyriakopoulos, A.T. Papastavrou, G.D. Panagiotou, M.D. Tzirakis, K.S. Triantafyllidis, M.N. Alberti, K. Bourikas, C. Kordulis, M. Orfanopoulos, A. Lycourghiotis, J. Mol. Catal. A 381 (2014) 9–15.
[17] R. Zugle, T. Nyokong, J. Mol. Catal. A 358 (2012) 49–57.
[18] L. Villén, F. Manjón, D. García-Fresnadillo, G. Orellana, Appl. Catal. B 69 (2006) 1–9.
[19] F. Manjón, M. Santana-Magaña, D. García-Fresnadillo, G. Orellana, Photochem. Photobiol. Sci. 9 (2010) 838–845.

[20] D. García-Fresnadillo, Y. Georgiadou, G. Orellana, A.M. Braun, E. Oliveros, Helv. Chim. Acta 79 (1996) 1222–1238.
[21] F. Manjón, L. Villén, D. García-Fresnadillo, G. Orellana, Environ. Sci. Technol. 42 (2008) 301–307.
[22] G. Orellana, M.C. Moreno-Bondi, D. García-Fresnadillo, M.D. Marazuela, in: G. Orellana, M.C. Moreno-Bondi (Eds.), Series Editor: O.S. Wolfbeis, Frontiers in Chemical Sensors: Novel Principles and Techniques. Springer Series on Chemical Sensors and Biosensors, Springer-Verlag, Berlin, 2005, pp. 189–225.
[23] G. Orellana, M.E. Jiménez-Hernández, D. García-Fresnadillo, Spanish Patent 2226576 to Photocatalytic material and method for water disinfection, 2003.
[24] M.L. Marín, L. Santos-Juanes, A. Arques, A.M. Amat, M.A. Miranda, Chem. Rev. 112 (2012) 1710–1750.
[25] Ch. Navntoft, P. Araujo, M.I. Litter, M.C. Apella, D. Férnandez, M.E. Puchulu, M.V. Hidalgo, M.A. Blesa, J. Sol. Energy Eng. 129 (2006) 127–134.
[26] J.L. Packer, J.J. Werner, D.E. Latch, K. McNeill, W.A. Arnold, Aquat. Sci. 65 (2003) 342–351.
[27] M.I. Burguete, R. Gavara, F. Galindo, S.V. Luis, Catal. Commun. 11 (2010) 1081–1084.
[28] D. Gryglik, J.S. Miller, S. Ledakowicz, Solar Energy 77 (2004) 615–623.
[29] J.S. Miller, Water Res. 39 (2005) 412–422.
[30] L. Carlos, D.O. Mártire, M.C. Gonzalez, J. Gomis, A. Bernabeu, A.M. Amat, A. Arques, Water Res. 46 (2012) 4732–4740.
[31] Confederación Hidrográfica del Ebro, Caracterización de las aguas superficiales y control de los retornos del riego en la cuenca del Ebro, 2006.
[32] R.A. Torres, F. Abdelmalek, E. Combet, C. Pétrier, C. Pulgarin, J. Hazard. Mater. 146 (2007) 546–551.
[33] Y. Barbieri, W.A. Massad, D.J. Díaz, J. Sanz, F. Amat-Guerri, N.A. García, Chemosphere 73 (2008) 564–571.
[34] L. Ferrando-Climent, N. Collado, G. Buttiglieri, M. Gros, I. Rodriguez-Roda, S. Rodriguez-Mozaz, D. Barceló, Sci. Total Environ. 438 (2012) 404–413.
[35] J.B. Quintana, S. Weiss, Th. Reemtsma, Water Res. 39 (2005) 2654–2664.
[36] E. Illés, E. Takács, A. Dombi, K. Gajda-Schrantz, G. Rácz, K. Gonter, L. Wojnárovits, Sci. Total Environ. 447 (2013) 286–292.
[37] I. Michael, A. Achilleos, D. Lambropoulou, V.O. Torrens, S. Pérez, M. Pétrovic, D. Barceló, D. Fatta-Kassinos, Appl. Catal. B 147 (2014) 1015–1027.
[38] M. Skoumal, R.M. Rodríguez, P.L. Cabot, F. Centellas, J.A. Garrido, C. Arias, E. Brillas, Electrochim. Acta 54 (2009) 2077–2085.
[39] F. Méndez-Arriaga, S. Esplugas, J. Giménez, Water Res. 42 (2008) 585–594.
[40] S.P. Sun, X. Zeng, A.T. Lemley, J. Mol. Catal. A Chem. 371 (2013) 94–103.
[41] J. Choina, H. Kosslick, Ch. Fischer, G.U. Flechsig, L. Frunza, A. Schulz, Appl. Catal. B 129 (2013) 589–598.
[42] F. Méndez-Arriaga, S. Esplugas, J. Giménez, Water Res. 44 (2010) 589–595.
[43] J. Madhavan, F. Grieser, M. Ashokkumar, J. Hazard. Mater. 178 (2010) 202–208.
[44] B. Zheng, Z. Zheng, J.B. Zhang, X.Z. Luo, J.Q. Wang, Q. Liu, L.H. Wang, Desalination 276 (2011) 379–385.
[45] Material Safety Data Sheetsfrom Sigma-Aldrich and Clearsynth, according to Regulation (EC) No. 1907/2006.
[46] S. Horikoski, A. Tokunaga, H. Hidaka, N. Serpone, J. Photochem. Photobiol. A 162 (2004) 33–40.
[47] M. Umar, F. Roddick, L. Fan, H.A. Aziz, Chemosphere 90 (2013) 2197–2207.
[48] E.M. Rodríguez, G. Fernández, N. Klamerth, M.I. Maldonado, P.M. Álvarez, S. Malato, Appl. Catal. B 95 (2010) 228–237.
[49] I. Gültekin, N.H. Ince, J. Environ. Manage. 85 (2007) 816–832.
[50] P.J. Chen, K.G. Linden, D.E. Hinton, Sh. Kashiwada, E.J. Rosenfeldt, S.W. Kullman, Chemosphere 65 (2006) 1094–1102.